

In situ measurements of liquid water content profiles in midlatitude stratiform clouds

A. V. Korolev,* G. A. Isaac, J. W. Strapp, S. G. Cober and H. W. Barker
Environment Canada, Toronto, Canada

ABSTRACT: Statistical characteristics of 584 liquid water content (LWC) profiles collected mainly in midlatitude supercooled stratiform frontal clouds during five field campaigns are presented. It has been found that the majority (55%) of liquid layers have thickness less than 500 m and the depth of these layers decreases with decreasing temperature. LWC profiles for thin cloud layers are usually close to quasi-adiabatic, whereas for thick clouds they are approximately constant with an average LWC value close to 0.14 g m^{-3} . Good agreement was observed between cumulative distributions for liquid water paths derived from *in situ* LWC profiles and those inferred in previous experiments from ground-based 37 GHz radiometers. Copyright © 2007 Crown in the right of Canada. Published by John Wiley & Sons, Ltd.

KEY WORDS LWC profiles; LWP

Received 13 March 2007; Revised 6 June 2007; Accepted 27 July 2007

1. Introduction

Knowledge of the vertical variability of cloud microphysical characteristics is important for a variety of reasons. The profile of liquid water content (LWC) partially governs the radiative transfer for cloudy atmospheres and thus ultimately Earth's radiation budget (e.g. Li and Barker, 2002; Barker and Räisänen, 2005). Information about LWC profiles improves our understanding of processes acting to form and maintain cloud systems and may lead to improvements in the representation of clouds in numerical models. Moreover, the vertical distribution of LWC and temperature inside supercooled clouds is important for estimating in-flight icing severity and aviation safety. Presently, *in situ* airborne measurements provide the most accurate information about cloud microphysical characteristics. This information can be used for verification of both numerical models and cloud remote-sensing techniques.

Statistical characteristics of vertical profiles of supercooled stratiform clouds collected during five field campaigns are presented here. Effort was focused on an analysis of the statistics for cloud geometric depth, liquid water path, vertical distribution of LWC, and temperature inside clouds.

2. Instrumentation

Measurements of LWC profiles were obtained using the National Research Council of Canada Convair-580

aircraft which was equipped with cloud microphysical sensing instruments provided and operated by Environment Canada (Isaac *et al.*, 1998, 2001a). The following set of aircraft instruments was used to characterize cloudy environments: (1) a Nevzorov probe (Sky Tech Research, Inc.) for measurements of LWC and total (ice + liquid) water content (TWC) (Korolev *et al.*, 1998); (2) a Particle Measuring Systems, Inc. (PMS) King probe for measurements of LWC (King *et al.*, 1978); (3) a Rosemount Icing Detector (RICE) (BF Goodrich Aerospace Sensors Division) for detecting the presence of supercooled liquid water with $\text{LWC} > 0.01 \text{ g m}^{-3}$ (Cober *et al.*, 2001a; Mazin *et al.*, 2001); (4) PMS OAP-2DC and OAP-2DP optical array probes for sizing and imaging cloud particles larger than approximately $100 \mu\text{m}$ and identifying the presence of drizzle and rain drops using image recognition analysis; (5) two Rosemount total-air temperature probes (model 102DJ1CG) (Lawson and Cooper, 1990; Friehe and Khelif, 1992) and one reverse-flow air-temperature probe (Rodi and Spyers-Duran, 1972); (6) a Rosemount 858 for measurements of wind gusts, altitude, and airspeed; and (7) a Litton 9100 IRS for measurements of position and altitude, and contributing to wind calculations. The liquid water path (LWP) for each cloud layer was computed from aircraft observations obtained by climbs or descents through the cloud layer. For this study, only the liquid fraction of condensed water in mixed-phase clouds was considered; the corresponding ice fraction of condensed water was disregarded. For simplicity, all clouds with $\text{LWC} > 0$ will be referred to hereafter as 'liquid', regardless of whether they contained ice particles or not.

The Nevzorov probe was chosen as the primary instrument for measurements of LWC. To avoid artifacts

* Correspondence to: A. V. Korolev, Environment Canada, 4905 Dufferin Street, Toronto, Ontario, M3H5T4 Canada.
E-mail: alexei.korolev@ec.gc.ca

and misinterpretation of data due to possible probe malfunctions, data from the Nevzorov probe were always compared to RICE, King probe, PMS FSSP, OAP-2DC and OAP-2DP data. Calculations of LWC from Nevzorov probe data were made following the procedure described by Korolev *et al.* (2003). Several studies have shown that ice particles may cause a response on the LWC sensor (e.g. Korolev *et al.*, 1998; Strapp *et al.*, 1999; Cober *et al.*, 2001b; Korolev and Strapp, 2002; Field *et al.*, 2004). The residual effect of ice on the LWC sensor is due to small amounts of heat removed from the sensor via impacts with ice particles. The effect is characterised by the residual coefficient $\alpha = W_{\text{liq}}^*/W_{\text{ice}}$, where W_{liq}^* is the response of the LWC sensor to ice particles with a corresponding ice water content W_{ice} . In practice, the residual coefficient is usually estimated as $\alpha = W_{\text{LWC}}/W_{\text{TWC}}$, where W_{LWC} and W_{TWC} are water contents measured in *ice* clouds (i.e. $\text{LWC} = 0$) by the LWC and TWC sensors, respectively. The value of α is thought to depend on the size, shape and bulk density of ice particles, air speed, air and sensor temperatures, and it has been shown to vary from 0.01 to 0.5. Large values of α have been observed in measurements near the cores of thunderstorms, and it has been speculated that they are the characteristic response of the probe to high concentrations of small ice particles and/or higher true airspeeds (Strapp *et al.*, 1999). In midlatitude frontal clouds, α is usually close to 0.18 (Korolev and Strapp, 2002; Field *et al.*, 2004). This value was used for this study.

3. Description of the dataset

Data used in this study were collected during five field campaigns: (1) the First Canadian Freezing Drizzle Experiment (CFDE 1) in March 1995 (Cober *et al.*, 2001c); (2) the Third Canadian Freezing Drizzle Experiment (CFDE 3) in December 1997–February 1998 (Isaac *et al.*, 1998); (3) the First Alliance Icing Research Study (AIRS1) December 1999–February 2000 (Isaac *et al.*, 2001b); (4) the Alliance Icing Research Study 1.5 (AIRS1.5) January 2003; and (5) the Second Alliance Icing Research Study (AIRS2) November 2003–February 2004 (Isaac *et al.*, 2005). During CFDE 1 flights were conducted over Newfoundland and the east coast of Canada, whereas during CFDE 3 and AIRS (1, 1.5 and 2) they were carried out over southern Ontario and Quebec.

The bulk of the data were sampled in stratiform clouds (St, Sc, Ns, As, Ac), associated with frontal systems. The air speed of the Convair-580 during sampling was approximately 100 m s^{-1} . Measurements were averaged over one-second time intervals. The data were obtained from 67 flights with typical durations of between 2 and 5 hours. Temperatures associated with the LWC profiles were limited to the range of 0°C to -35°C with altitudes ranging from the surface to 7 km.

Profiles were accomplished by using both spiral and en-route climbs and descents. Aircraft climb or descent

rates during vertical soundings ranged from 2 m s^{-1} to 18 m s^{-1} but were typically approximately 5 m s^{-1} . These rates correspond to approximately 1° , 10° , and 3° glide slopes of the Convair 580, respectively. In order to reduce the effect of spatial inhomogeneity of cloud microstructure, soundings for deep clouds with geometric thickness $\Delta Z > 1.5 \text{ km}$ were carried out during spiral ascent or descent. The radius of Convair spiral circles was typically three kilometres.

The horizontal scale over which vertical soundings were accomplished depended on ΔZ and varied from 1 km to 10 km. Due to their large horizontal extent, such vertical soundings should be considered as *quasi-vertical*. The vertical distribution of LWC obtained from individual *quasi-vertical* profiles may be different from that obtained from *truly* vertical ones due to spatial variations in LWC. It can be shown, however, that by averaging over large enough numbers of *truly* vertical and *quasi-vertical* soundings, the two methods yield the same average characteristics. This enables one to conclude that for the large number of vertical profile samples used in this study, horizontal inhomogeneity of LWC has a limited effect on the results discussed below.

The total number of separately analysed stratiform layers was 584. Two cloud layers were considered distinct if the vertical distance between the top of the lower layer and the base of the upper layer exceeded 50 m. Otherwise, the two segments were considered to be a continuous single layer. In order to avoid misidentifying cloud fragments, which are typically observed near cloud boundaries, cloud layers with $\Delta Z < 50 \text{ m}$ were excluded from this analysis. The sensitivity threshold for the detection of liquid clouds was chosen as 0.005 g m^{-3} . Clouds with $\text{LWC} < 0.005 \text{ g m}^{-3}$ were disregarded and considered to be clear air.

The liquid clouds considered here were composed mainly of cloud droplets with diameters less than $50 \mu\text{m}$. In some clouds a certain fraction of liquid water may be related to precipitation-sized particles. However, cases with precipitation, observed below cloud bases, were excluded from this analysis. Cober *et al.* (2001c) provided some vertical profile characteristics for cloud layers with supercooled drops greater than $100 \mu\text{m}$ in diameter.

Since the five flight campaigns were carried out during cold seasons, most of the clouds sampled were supercooled. Therefore, results presented here may not be suitable for verification of numerical models and remote-sensing retrieval algorithms related to warm stratiform frontal clouds.

4. Results

4.1. Distribution of LWC within cloud layers

Theoretical calculations suggest that for clouds formed by adiabatic lifting, LWC increases with altitude and is a unique function of height above cloud base. It can be shown that for displacements of a few hundred metres,

changes in β_{ad} , the vertical gradient of adiabatic LWC, are less than a few percent, depending on temperature and pressure, and β_{ad} may be considered to be approximately constant. Therefore, LWC is expected to change linearly with altitude for relatively thin clouds ($\Delta Z < 500$ m).

In real clouds, LWC values are lower than the adiabatic prediction because of entrainment of drier air, mixing, precipitation fallout and radiative heating/cooling. As Figure 1 shows, LWC can both increase (Figure 1(a)) and decrease (Figure 1(b)) towards cloud top, or may display several local maxima (Figure 1(c)). The local maxima in Figure 1(c) may be related to the horizontal inhomogeneity of LWC.

Figure 2 shows average LWC profiles calculated for layers with $\Delta Z < 500$ m, $500 < \Delta Z < 1000$ m and $\Delta Z > 1000$ m. Since cloud depth and LWC vary over wide ranges, elevation above cloud base was normalized to cloud depth (ΔZ_{norm}), and LWC was normalized to maximum LWC (W_{max}). As seen from Figure 2(a), LWCs change nearly linearly in the lower to middle parts

of clouds with $\Delta Z < 500$ m, and have a distinct maximum at ΔZ_{norm} approximately equal to 0.8. Figure 2(b) and (c) show that the average LWC profile for cloud layers with depths over 500 m have approximately constant LWC for $0.4 < \Delta Z_{norm} < 0.9$.

Figure 3 shows the frequency distribution of the maximum observed LWC (at ~ 100 m horizontal averaging scale) for each supercooled cloud layer. The overall maximum LWC observed was 1.0 g m^{-3} while the mean and median were 0.32 g m^{-3} and 0.31 g m^{-3} , respectively. It can be seen in Figure 4 that the average LWC in cloud layers was found to be almost independent of cloud depth for clouds with $\Delta Z > 500$ m, and it is approximately equal to 0.14 g m^{-3} .

4.2. Thickness of supercooled cloud layers

The depth of continuous supercooled cloud layers varies from 50 metres (the threshold minimum for this study) to a few kilometres. Figure 5 shows the frequency

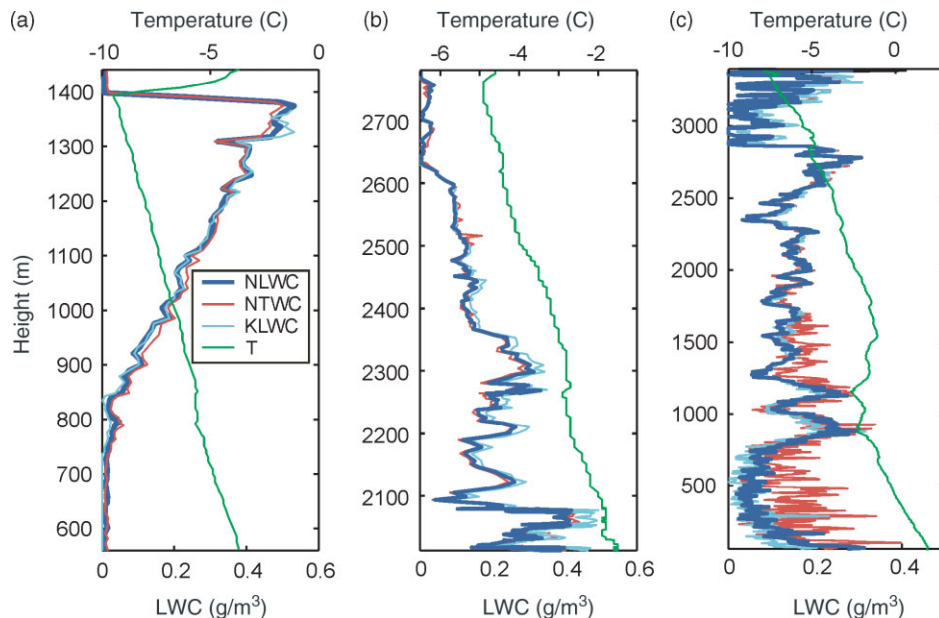


Figure 1. Different types of LWC profiles measured in stratiform clouds by three instruments: Nevzorov liquid water probe (NLWC); Nevzorov total water probe (NTWC); King hot wire probe (KLWC). (a) St-Sc, 15 December 1995 over southern Ontario; (b) Ns, 22 March 1995 over Newfoundland; (c) Ns, 11 November 2003 over southern Ontario.

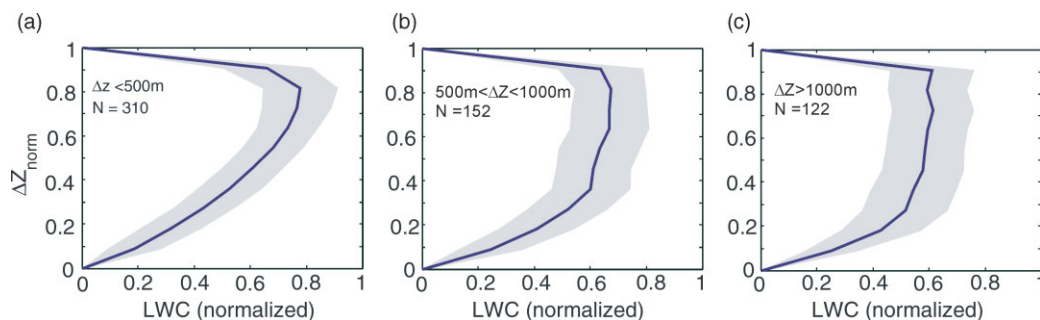


Figure 2. Average LWC profiles for stratiform cloud layers when: (a) $\Delta Z < 500$ m; (b) $500 \text{ m} < \Delta Z < 1000$ m; and (c) $\Delta Z > 1000$ m. LWC was normalized to the maximum value in each profile, and distance above base was normalized to the depth of the cloud layer. Grey shaded areas show averages \pm standard deviation of LWC data.

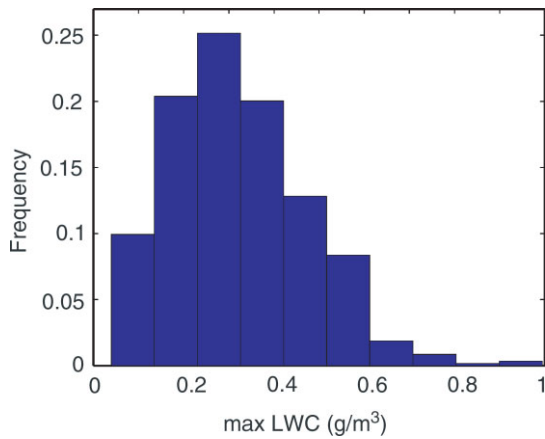


Figure 3. Frequency distribution of maximum LWC for stratiform cloud layers at intervals of 0.1 g m^{-3} . Note that these values pertain to a horizontal resolution of 100 m.

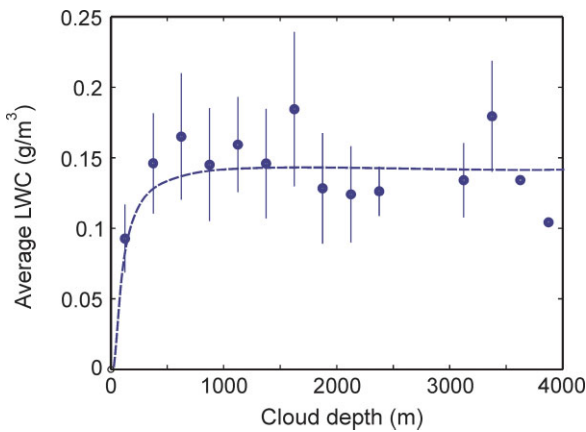


Figure 4. LWC averaged over a cloud depth versus depth of cloud. Dots represent average LWC in cloud layers as a function of cloud depth. Vertical bars indicate corresponding standard deviations.

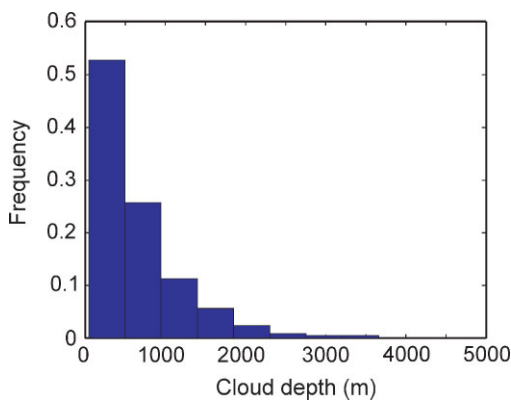


Figure 5. Frequency of occurrence of depth of supercooled stratiform cloud layers in intervals of 500 m.

distribution of supercooled liquid layer depths ΔZ . More than 50% of cloud layers have depths less than 500 m, and about 80% have $\Delta Z < 1 \text{ km}$. The maximum thickness of a continuous liquid layer was found to be 4500 m. Figure 1(c) shows the LWC profile for a deep cloud layer with $\Delta Z \sim 3500 \text{ m}$ and illustrates

the frequently observed situation of multiple distinct local maxima of LWC for deep continuous liquid cloud layers.

Figure 6 shows frequency distributions of cloud depths stratified by different mean cloud temperature intervals. Note that ΔZ has a tendency to decrease with decreasing temperature. Distributions for narrow temperature ranges resemble gamma distributions that behave like power laws for small ΔZ , while the overall distribution is very close to an exponential. Noting that cloud optical depth is related approximately linearly to ΔZ , the results shown in Figure 6 agree quite well with overcast cloud optical depths inferred from surface pyranometer data collected across Canada (Barker *et al.*, 1998). Figure 7 shows the dependence of average ΔZ on the layer mean temperature and illustrates that the thickness of stratiform cloud decreases with decreasing temperature. Thus, below -25°C stratiform clouds were found to form thin layers having a depth usually no more than 100 m. The overall average and median depths

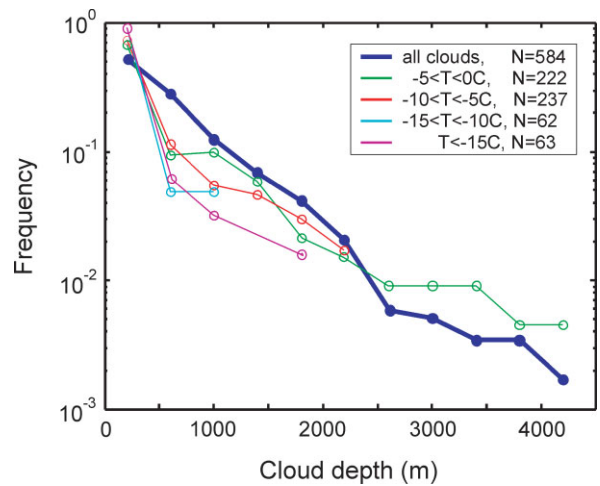


Figure 6. Frequency of occurrence of depth of stratiform layers in 400 m bins, for different temperature intervals. Thick blue line is for the distribution shown in Figure 5.

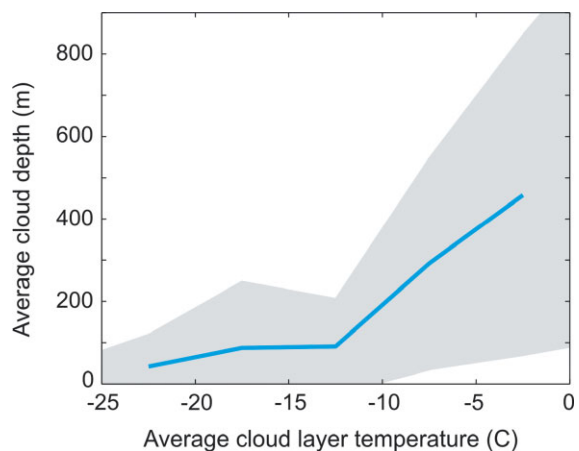


Figure 7. Average continuous cloud thickness of supercooled liquid layers versus corresponding average temperature of the layer. Shaded area indicates standard deviation of cloud depth.

of supercooled cloud layers were 660 m and 470 m, respectively.

4.3. Temperature distribution in supercooled cloud layers

The air temperature in most supercooled liquid layers decreases towards cloud top. Some cloud layers, however, may have an embedded temperature inversion where temperature increases with height (see Figure 1(c)). This proves to be generally true in most frontal cloud layers. The fractions of cloud layers where temperature at cloud top (T_{top}) is colder than, equal to, or warmer than at cloud base (T_{base}) are 0.66, 0.17, and 0.17, respectively. The temperatures T_{top} and T_{base} were classified as 'equal' if $|T_{\text{top}} - T_{\text{base}}| < 0.5^\circ\text{C}$. It was found that T_{top} for deep cloud layers ($\Delta Z > 2$ km) is usually warmer than -10°C .

4.4. Liquid water path

Figure 8 shows the cumulative probability of liquid water path (LWP) derived from *in situ* measurements of LWC in cloud layers (blue circles). Liquid water path is the total amount of liquid water per unit area in the column of air from cloud base to top. In the case of the aircraft data, LWP is estimated by integrating the product of LWC and height change in each one-second data interval through the cloud. The results are expressed in the figure in terms of the probability of LWP exceeding a given value. The figure includes a comparison to LWP inferred from ground-based vertically pointing 37 GHz microwave radiometer measurements (red circles) collected over one winter season near Toronto, Canada (adapted from Koldaev *et al.*, 1999). The radiometer provides a continuous estimate of LWP in a column above

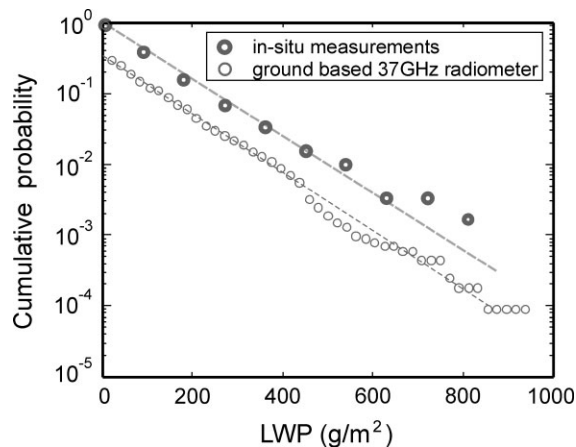


Figure 8. Cumulative frequency of occurrence of the liquid water path (LWP) for stratiform cloud layers (blue circles), and probability of LWP based on ground-based measurements inferred from 37 GHz. radiances (Koldaev *et al.*, 1999) (red circles). Values represent the fraction of cases exceeding the LWP path value. Note that ground-based values are for all-sky conditions and thus have clear skies factored in. Overall, the good agreement between the slopes of the lines is encouraging for it suggests that LWP retrievals from surface-based radiometer data, which are far less expensive to obtain than those from aircraft, are accurate.

the radiometer, and therefore can contain LWP estimates from multiple layers. Nevertheless the slopes of the two distributions are quite similar. The offset between the two curves is due to the fact that the radiometer data are absolute probabilities that include periods of no liquid cloud (about 65% of the time), whereas the airborne data are conditional probabilities where cloud must be present.

Despite the fact that the aircraft dataset contains some LWC profiles from the Canadian Arctic collected during FIRE-ACE (First ISCCP Regional Experiment–Arctic Cloud Experiment), the majority of airborne *in situ* and remotely sensed radiometric data were collected from more southerly climatic zones that have, presumably, similar distributions of LWP (see Barker *et al.*, 1998).

Figure 9 shows the dependence of LWP on ΔZ . As seen in this figure, LWP is approximately a linear function of ΔZ , and can be described as

$$LWP \cong 0.14\Delta Z, \quad (1)$$

where ΔZ is in metres, and LWP in g m^{-2} . This is completely consistent with the result presented in Figure 4 in which average LWC for cloud layers with $\Delta Z > 500$ m, regardless of depth, is 0.14 g m^{-3} . It is worth mentioning that the linear dependence of LWP versus ΔZ is different from the adiabatic prediction in which LWP is proportional to ΔZ^2 (which is the case for shallow stratiform layers with $\Delta Z < 500$ m).

5. Discussion

This study of wintertime stratiform frontal clouds in southern Canada has shown that the depths of continuous liquid layers may reach 3–4 km (see Figures 5 and 6), but that about 80% of these clouds have liquid layer depths less than 500 m. Regardless of the total cloud depth, profiles of cloud water content behave quasi-linearly up to about 500 m above cloud base. Analysis of Figures 2 and 4 suggests that the average value of LWC stays approximately constant above 500 m for clouds that are thicker than about 500 m.

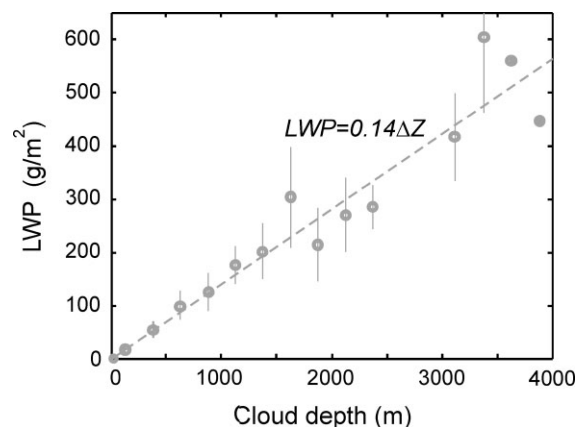


Figure 9. Dots represent average liquid water path (LWP) of supercooled stratiform cloud layers as a function of cloud depth. Thin vertical lines indicate standard deviations.

Liquid water profiles in thick clouds are essentially non-adiabatic with water contents near the tops of deep cloud layers (i.e. $\Delta Z > 2$ km) being typically 5 to 10 times smaller than adiabatic. The LWC profile in deep cloud layers typically has several distinct maxima (Figure 1(c)). Such a vertical structure of LWC suggests that the vertical transport of cloud parcels in deep stratiform clouds is limited. In other words cloud parcels may not travel from cloud base to cloud top, as they do in shallow stratocumulus layers, but rather oscillate around certain levels. Such oscillations may be arranged as closed cells generated by gravity waves or wind shear, which are characteristic features of frontal systems. Figure 10 shows a conceptual diagram of a dynamic structure explaining multi-maximum LWC profiles in deep frontal layers. Each of these cells may generate a quasi-adiabatic profile of LWC. The characteristic vertical extent of such cells, ΔH_c , can be estimated from the maximum LWC, which will be reached in the upper part of the cells, as follows:

$$\Delta H_c = W_{\max} / \beta_{\text{ad}}. \quad (2)$$

As found in Figure 3, the average value of $W_{\max} = 0.3 \text{ g m}^{-3}$. Assuming $\beta_{\text{ad}} = 1.2 \times 10^{-3} \text{ g m}^{-3} \text{ m}^{-1}$ at $T = -5^\circ\text{C}$ and $P = 700 \text{ mb}$, (2) yields $\Delta H_c \sim 250 \text{ m}$. Taking into account the non-adiabatic nature of LWC due to mixing, precipitation fallout, etc., the actual size of the cells will probably be deeper than this, and perhaps more consistent with the depth of quasi-adiabatic single layers $\Delta Z \sim 500 \text{ m}$.

6. Conclusions

Based on the analysis of 584 supercooled cloud layers, the following conclusions have been obtained:

- (1) The majority (55%) of liquid layers in midlatitude stratiform clouds have thicknesses $\Delta Z < 500 \text{ m}$. These layers tend to have a quasi-linear LWC profile. Deeper liquid layers ($\Delta Z > 500 \text{ m}$) also have quasi-linear profiles in their lowest 500 m, but transition to a near constant LWC in their central and upper regions.
- (2) The LWC averaged over cloud depth (\bar{W}), for cloud layers with $\Delta Z > 500 \text{ m}$ does not depend on ΔZ

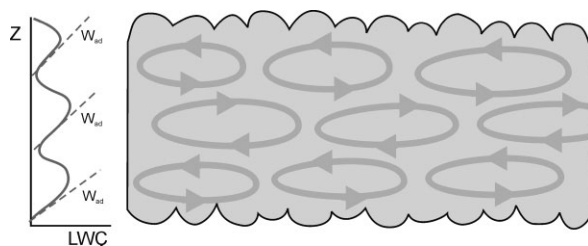


Figure 10. Conceptual diagram portraying the formation of multi-maxima LWC profiles in deep stratiform clouds.

and is approximately equal to 0.14 g m^{-3} ; for thinner clouds with $\Delta Z < 500 \text{ m}$, however, $\bar{W} / \Delta Z \cong 1 \text{ g m}^{-3} \text{ km}^{-1}$.

- (3) The depth of liquid cloud layers decreases with decreasing average layer temperature. Typically for cold cloud layers with an average temperature $T = -25^\circ\text{C}$, their average depth does not exceed 100 m.
- (4) Good agreement was observed in the slope of cumulative distributions of LWP derived from *in situ* LWC profiles and those inferred in previous experiments from ground-based 37 GHz radiometers.
- (5) Deep stratiform liquid layers usually have LWC profiles with multiple local maxima. Such profiles may be explained by multi-cellular circulations with each cell having a vertical dimension on the order of a few hundred metres.

Acknowledgements

All the measurements reported in this paper were made using the National Research Council Canada (NRC) Convair-580. The authors would like to acknowledge the efforts of their NRC colleagues in these airborne experiments. In addition to the financial contributions of Environment Canada and NRC, funding was provided by several agencies including the Canadian National Search and Rescue Secretariat, Transport Canada, the US Federal Aviation Administration, and the Boeing Commercial Airplane Group.

References

- Barker HW, Räisänen P. 2005. Radiative sensitivities for cloud structural properties that are unresolved by conventional GCMs. *Q. J. R. Meteorol. Soc.* **131**: 3103–3122.
- Barker HW, Curtis TJ, Leontieva E, Stamnes K. 1998. Optical depth of overcast cloud across Canada: Estimates based on surface pyranometer and satellite measurements. *J. Climate* **11**: 2980–2994.
- Cober SG, Isaac GA, Korolev AV. 2001a. Assessing the Rosemount Icing Detector with *in situ* measurements. *J. Atmos. Oceanic Technol.* **18**: 515–528.
- Cober SG, Isaac GA, Korolev AV, Strapp JW. 2001b. Assessing cloud-phase conditions. *J. Appl. Meteorol.* **40**: 1967–1983.
- Cober SG, Isaac GA, Strapp JW. 2001c. Characterizations of aircraft icing environments that include supercooled large drops. *J. Appl. Meteorol.* **40**: 1984–2002.
- Field PR, Hogan RJ, Brown PRA, Illingworth AJ, Choullarton TW, Kaye PH, Hirst E, Greenaway R. 2004. Simultaneous radar and aircraft observations of mixed-phase cloud at the 100 m scale. *Q. J. R. Meteorol. Soc.* **130**: 1877–1904.
- Friehe CA, Khelif D. 1992. Fast-response aircraft temperature sensors. *J. Atmos. Oceanic Technol.* **9**: 784–795.
- Isaac GA, Cober SG, Korolev AV, Strapp JW, Tremblay A, Marcotte DL. 1998. 'Overview of the Canadian Freezing Drizzle Experiment I, II and III.' Pp. 447–450 in Preprints, Conf. on Cloud Physics, Everett, WA, USA. American Meteorol. Soc.
- Isaac GA, Cober SG, Strapp JW, Korolev AV, Tremblay A, Marcotte DL. 2001a. Recent Canadian research on aircraft in-flight icing. *Can. Aeronautics and Space J.* **47**: 213–221.
- Isaac GA, Cober SG, Strapp JW, Hudak D, Ratvasky TP, Marcotte DL, Fabry F. 2001b. 'Preliminary results from the Alliance Icing Research Study (AIRS).' AIAA 39th Aerospace Sciences Meeting and Exhibit, 8–11 Jan 2001, Reno, Nevada, USA. AIAA 2001-0393, 12 pp.
- Isaac GA, Ayers JK, Bailey M, Bissonnette L, Bernstein BC, Cober SG, Driedger N, Evans WFJ, Fabry F, Glazer A, Gulpepe I, Hallett J, Hudak D, Korolev AV, Marcotte D, Minnis P, Murray J, Nguyen L, Ratvasky TP, Reehorst A, Reid J, Rodriguez P, Schneider T,

- Sheppard BE, Strapp JW, Wolde M. 2005. 'First results from the Alliance Icing Research Study II.' AIAA 43rd Aerospace Sciences Meeting and Exhibit, 11–13 Jan 2005, Reno, Nevada, USA. AIAA 2005-0252.
- King WD, Parkin DA, Handsworth RJ. 1978. A hot-wire liquid water device having fully calculable response characteristics. *J. Appl. Meteorol.* **17**: 1809–1813.
- Koldaev A, Low TB, Strapp JW. 1999. 'Microwave measurements of cloud liquid water path and average in-cloud temperature at King City, Ontario, winter 96/97.' Transport Canada Report TP14104, March 1999, 94 pp.
- Korolev AV, Strapp JW. 2002. 'Accuracy of measurements of cloud ice water content by the Nevzorov probe.' AIAA 40th Aerospace Sciences Meeting and Exhibit, 14–17 Jan 2002, Reno, Nevada, USA. AIAA 2002-0679, 9 pp.
- Korolev AV, Strapp JW, Isaac GA, Nevzorov AN. 1998. The Nevzorov airborne hot-wire LWC–TWC probe: Principle of operation and performance characteristics. *J. Atmos. and Oceanic Technol.* **15**: 1495–1510.
- Korolev AV, Isaac GA, Cober SG, Strapp JW, Hallett J. 2003. Microphysical characterization of mixed-phase clouds. *Q. J. R. Meteorol. Soc.* **129**: 39–65.
- Lawson RP, Cooper WA. 1990. Performance of some airborne thermometers in clouds. *J. Atmos. Oceanic Technol.* **7**: 480–494.
- Li J, Barker HW. 2002. Accounting for unresolved clouds in a 1D infrared radiative transfer model. Part II. Horizontal variability of cloud water path. *J. Atmos. Sci.* **59**: 3321–3339.
- Mazin IP, Korolev AV, Heymsfield A, Isaac GA, Cober SG. 2001. Thermodynamics of icing cylinder for measurements of liquid water content in supercooled clouds. *J. Atmos. Oceanic Technol.* **18**: 543–558.
- Rodi AR, Spyers-Duran PA. 1972. Analysis of time response of airborne temperature sensors. *J. Appl. Meteorol.* **11**: 554–556.
- Strapp JW, Chow P, Maltby M, Bezer AD, Korolev AV, Stromberg I, Hallett J. 1999. 'Cloud microphysical measurements in thunderstorm outflow regions during Allied/BAE 1997 flight trials.' AIAA 37th Aerospace Sciences Meeting and Exhibit, 11–14 Jan 1999, Reno, Nevada, USA. AIAA 99-0498, 10 pp.